ASTRONOMY & ASTROPHYSICS
SUPPLEMENT SERIES

Astron. Astrophys. Suppl. Ser. **47**, 601-609 (1982)

A Westerbork survey of clusters of galaxies. XIV. Abell 779 and Abell 1314

A. S. Wilson ([1, 3]) and J. P. Vallée ([2, 3])

([1]) Astronomy Program, University of Maryland, College Park, MD 20742, U.S.A.
([2]) Herzberg Institute of Astrophysics, National Research Council of Canada, Ottawa, ONT K1A 0R6, Canada
([3]) Sterrewacht, Huygens Laboratorium, Wassenaarserweg 78, 2300 RA Leiden, The Netherlands

Received August 3, accepted September 22, 1981

Summary. — The clusters of galaxies Abell 779 and Abell 1314 have been observed with the Westerbork telescope at 610 MHz (λ 49 cm) to a resolution of about 1 arc min and sensitivity (5 × r.m.s.) near 10 mJy. 111 radio sources have been detected in all. Optical identification shows that 5 or 6 radio sources are probably associated with bright cluster galaxies. The differential count of those radio sources apparently not associated with cluster galaxies has been derived in the flux density range 10-500 mJy, and is found to be similar to that obtained at 408 MHz in the 5C 5 survey.

Key words : Clusters of galaxies — radio sources survey — source counts.

1. **Introduction.** — Radio studies of clusters of galaxies with aperture-synthesis instruments are of value in simultaneously surveying a large number of galaxies, in deciding whether the radio properties of galaxies in rich clusters differ from those in poor clusters or in the field and in probing the intracluster medium through its interaction with the radio components. In this paper, we report results at λ 49 cm on the clusters Abell 779 and 1314. These clusters were selected from the survey of Owen (1974), who suggested that several galaxies in these clusters could be radio emitters, but his resolution of 10 arc min. was too low to define the association in detail. As well as identifying a number of radio sources with cluster galaxies, we report the counts of background radio sources in these directions to about 10 mJy. Our study is similar to earlier Westerbork surveys of other clusters of galaxies (e.g. Harris and Miley, 1978; Harris *et al.*, 1980; Valentijn, 1980 and references therein). Westerbork and VLA results on the head-tail radio galaxies IC 708 and IC 711 in Abell 1314 have been presented elsewhere (Vallée and Wilson, 1976; Wilson and Vallée, 1977; Vallée *et al.*, 1979, 1981). Throughout the paper we adopt the Hubble constant $H_0 = 50$ km s^{-1} Mpc^{-1}.

2. **Observations and reduction.** — The observations were made with the Westerbork Synthesis Radio Telescope (Högbom and Brouw, 1974; Baars *et al.*, 1973) at λ 49 cm. At the time of the observations, the instrument consisted of twelve 25 meter paraboloids along an E-W line. Correlation of the signals from each of the two moveable antennas (A and B) with each of the ten fixed ones (0 to 9) yielded twenty simultaneous baselines ranging from 72 to 1440 meters. Table I lists the pertinent observational parameters for each cluster. Calibration was achieved by observations of 3C 48, 3C 147 and 3C 309.1 whose assumed positions and flux densities were as given by Jaffe *et al.* (1976).

Maps of the brightness distributions in Stokes parameters *I*, *Q*, *U* and *V* were made by Fourier transformation. No significant polarization was detected; the 3 × r.m.s. upper limit on linear or circular polarization of a point source is $\simeq 600/S$ % where *S* is the map flux in mJy.

The maps of total intensity were « cleaned » (Högbom, 1974), contour plots prepared and a list of suspected sources with peak map flux densities $S_{peak} > 5 \times$ r.m.s. noise and within 1°25(= 3.0 Mpc for Abell 779, $z=0.0227$, Hintzen *et al.* 1978; = 4.4 Mpc for Abell 1314, $z = 0.0338$, Coleman *et al.*, 1976), of the field center was compiled. Care was taken to avoid any weak residual grating responses by visual comparison with the contour diagrams of the original maps. For the purposes of source parameter extraction, we divided the sources into two categories. The first category is designated « simple sources » ; such sources are point-like (U) or only slightly broader than the restoring beam (R). The second category is referred to as « complex » (C) ; these sources are well resolved and exhibit structure in their brightness distributions.

2.1 Simple sources. — A 2-dimensional Gaussian function was fitted to the 5 × 5 matrix of points surrounding the source and a comparison Gaussian to the instrumental response. The fitting program derives the position of the centroid of the brightness distribution and also the integrated map flux S_{int} via the relation

Send offprint requests to : A. S. Wilson, Astronomy Program, University of Maryland, College Park, MD 10742, U.S.A.

$$S_{int} = \frac{\theta_1 \theta_2}{\theta_{1B} \theta_{2B}} S_{peak} \quad (1)$$

where S_{peak} is the peak map flux density of the source (determined from the Gaussian fit), θ_1 and θ_2 are the half power widths of the major and minor axes of the Gaussian fitted to the source while θ_{1B} and θ_{2B} are the corresponding values for the antenna pattern. To derive sky flux densities, S_{int} was divided by the power pattern $P(R)$ of the individual antennas which may be described by the form :

$$P(R) = 1.00 + 0.11\,R - 2.13\,R^2 + 1.51\,R^3 - 0.28\,R^4 \quad (2)$$

where R is the distance of the source from the field centre in degrees. For example, when R = 0°.5, 1° and 1°.25, $P(R)$ = 0.69, 0.21 and 0.07 respectively.

In order to decide whether a source was resolved, we have adopted the criterion of Willis *et al.* (1976). The source was defined as extended if the area of the fitted elliptical Gaussian divided by the corresponding area of the synthesised antenna pattern differed from unity by more than twice the r.m.s. error. The criterion for resolution becomes (equation (3) of Willis *et al.*)

$$\frac{\theta_1 \theta_2}{\theta_{1B} \theta_{2B}} - 1 \geqslant \frac{2.29 \times \text{r.m.s. noise (mJy)}}{S_{peak}(\text{mJy})}. \quad (3)$$

According to Willis *et al.* (1976), use of equation (3) implies an ~ 2 % chance that a source will be incorrectly classified. For sources satisfying equation (3), deconvolved FWHM sizes and the position angle of the major axis were derived from formulae given by Wild (1970). Equation (3) gives no information on the reality of apparent extension along the minor axis of the source. We have followed the *ad hoc* criterion that the deconvolved minor axis sizes are listed only when they are greater than half the beamwidth in that direction (i.e. $26(1 - \cos^2 \delta \cos^2 (PA + 90°))^{-1/2}$ arc secs.

As most extended extragalactic sources show double structure, we have also derived the separation θ_{dp} of two equal point sources which corresponds to the deconvolved size along the major axis. To do this, the deconvolved Gaussian half width along the major axis θ_G, was first converted into its east-west equivalent, $\theta_{G,E-W}$:

$$\theta_{G,E-W} = \theta_G (1 - \cos^2 \delta \cos^2 PA)^{1/2} \quad (4)$$

where δ is the declination and PA the position angle of the major axis of the source. Next, we converted $\theta_{G,E-W}$ into the equivalent east-west separation of two equal point sources $\theta_{dp,E-W}$ using the empirical relationship found by Willis *et al.* (1976) :

$$\frac{\theta_{dp,E-W}}{\theta_{2B}} = \frac{-0.11 + \sqrt{1.21 \times 10^{-2} - 5.84(0.2 - \theta_{G,E-W}/\theta_{2B})}}{2.92} \quad (5)$$

where θ_{2B} is the east-west half width of the instrumental response. Finally $\theta_{dp,E-W}$ was converted into the desired separation of two equal point sources along the major axis :

$$\theta_{dp} = \theta_{dp,E-W} (1 - \cos^2 \delta \cos^2 PA)^{-1/2}. \quad (6)$$

2.2 COMPLEX SOURCES. — Sources larger than ~ 2 beamwidths show structure and are too complex for their fluxes and angular sizes to be determined by the Gaussian fit algorithm. The total map flux of such sources was derived by summation of the CLEAN components and then converted to sky fluxes by dividing by $P(R)$. Angular sizes for these sources were estimated from the contour plots.

3. **Errors in source parameters.** — 3.1 SIMPLE SOURCES. — The error in the right ascension of an unresolved source was derived from the empirical relationship found by Willis *et al.* (1976) using Monte Carlo trials. The declination error is simply a factor cosec δ larger than that in right ascension. The error in the map flux density follows the usual equation :

$$\Delta S_U = \sqrt{A^2 + (BS_{peak})^2}\ \text{mJy} \quad (7)$$

where $A \simeq$ 1.8-2.0 and B = 0.015. In equation (7), the first term on the R.H.S. results from noise while the second takes account of phase and gain instabilities in the telescope.

Following Willis *et al.*, we have taken the position error of a resolved source to be = S_{int}/S_{peak} × the position error for an unresolved source with the same peak flux density. The error in the integrated flux was calculated from

$$\Delta S_R = \sqrt{(\Delta S_U)^2 + C^2} \quad (8)$$

with C = 2.1-2.3 mJy (see Willis *et al.*, 1976).

3.2 COMPLEX SOURCES. — The error in the integrated flux density of a complex source was taken to be :

$$\Delta S_C = \sqrt{(NA)^2 + (BS_{peak})^2} \quad (9)$$

(see Willis *et al.*, 1976), where N is the number of beam areas covered by the source.

Equations (7), (8) and (9) refer to the error in the map flux density. This error was then divided by $P(R)$ and the result combined in quadrature with the errors from uncertainty in $P(R)$ and in the delay envelope, to yield the final error in the integrated sky flux density. The error in $P(R)$ was taken to be 10 R % where R is in degrees (Valentijn, 1980). The effects of the delay envelope are not well studied but the attenuation increases with increasing distance from the field center. We estimate that the contribution to the uncertainty in flux is ~ 4 % when 0°.5 < R < 1°.25.

4. **Results.** — Table II (III) contains 55 (56) sources within 1°.25 of the field center of Abell 779 (Abell 1314). The sources are listed down to a limiting *peak* map flux density of 5 × r.m.s. noise, which is about 9 mJy for Abell 779 and about 10 mJy for Abell 1314. The format of tables II and III is as follows :

Column 1 : The name of the source in a modified Parkes system nomenclature.
Column 2 : Right ascension (1950.0) and its error.
Column 3 : Declination (1950.0) and its error.

Column 4 : Attenuation by the power pattern of the individual antennas = $1/P(R)$.
Column 5 : Sky flux density at λ 49 cm and its error.
Column 6 : Radio Structure : U = Unresolved ; R = Resolved ; C = Complex (see Section II).

The catalog for Abell 1314 may be incomplete in two small regions. The first is a rectangular area of extent 1 arc min. in declination and 3 arc min. in right ascension centered at approx $\alpha = 11^h30^m54^s$, $\delta = 49°20'.5$. The second has coordinates $\alpha = 11^h32^m40^s$, $\delta = 49°17'$ and is $\sim$ 2 arc min. in size. In both regions, extended features with peak map flux density $\sim$ 12 mJy are found (see Fig. 1 of Vallée and Wilson, 1976). We suspect them to be residual sidelobes of 1131+49W4 = IC 708 or 1132+49W2 = IC 711 but cannot rule out the possible existence of real emission.

Table IV lists those sources which are classified as resolved (R) or complex (C) (see Section 2). The format of table IV is :

Column 1 : The name of the source.
Column 2 : Position angle of the major axis of the source (PA).
Column 3 : Gaussian size of the source along its major axis (θ_G).
Column 4 : Gaussian size of the source along its minor axis ($\theta_{G,min}$).
Column 5 : Separation of the equal double point source model (θ_{dp}).

Figure 1 shows radio contour maps for some extended and/or closely grouped sources. Sources in the central region of Abell 1314, including the head-tail radio galaxies 1131+49W4 = IC708 and 1132+49W2 = IC711 are not given here since maps of this region have been presented elsewhere (Vallée and Wilson, 1976 ; Wilson and Vallée, 1977).

An attempt was made to identify the radio sources with optical objects to the limit of the Palomar Sky Survey (PSS) prints. Positions of optical objects near to the radio sources were measured from the PSS (to an accuracy of $\pm$ 1″) by means of an X-Y measuring machine of the Herzberg Institute of Astrophysics and checked with the *Coradigraph* measuring machine of the Royal Greenwich Observatory. However, because of the relatively low accuracy of the radio positions, the number of identifications was only slightly in excess of the expected number of coincidences by chance (see e.g. McEwan *et al.*, 1975 ; Bergamini *et al.*, 1973). For this reason, we present in table V only the identifications with bright ($m_p < 16$) possible or probable members of Abell 779 or Abell 1314. The format of table V is :

Column 1 : The name of the source.
Column 2 : The apparent photographic magnitude of the galaxy from Zwicky and Herzog (1963).
Column 3 : The cluster with which the galaxy is probably or possibly associated.
Column 4 : The galaxy type.
Column 5 : The absolute photographic magnitude.
Column 6 : The monochromatic radio power at 610 MHz.
Column 7 : The linear size of the radio source.
Column 8 : The difference between the radio and optical right ascensions.
Column 9 : The difference between the radio and optical declinations.
Column 10 : Comments.

Some notes on individual galaxies follow :

NGC 2823. Previously this galaxy was considered the identification of OK 327 = 0916+34W2 (e.g. Grueff and Vigotti, 1971), but VLA observations by Fomalont and Bridle (1978) show the radio source to be double and displaced from NGC 2823. 0916+34W2 is probably unrelated to NGC 2823 or Abell 779.

0916 + 33W6 = NGC 2831/NGC 2832 (Fig. 1c). Although formally unresolved according to our criterion (Section 2), this radio source does appear extended roughly NW-SE on a contour map (Fig. 1c). The best estimate of the radio source position lies in between the bright elliptical NGC 2832 and NGC 2831 ; these two galaxies form a double system in a halo (Zwicky and Herzog, 1963). The direction of radio source elongation seems similar to that of the optical halo. Hintzen *et al.* (1978) found that the radial velocity of NGC 2831 is 1834 km s^{-1} less than the mean for Abell 779. However they consider the galaxy to be a probable cluster member because of its apparent close association with NGC 2832, a cluster galaxy.

0916 + 33W7 (Fig. 1d). A $15^m.3$ spiral (?) galaxy lies within the extension of the radio contours to the NE but is displaced from their peak ($\alpha_r - \alpha_0 = -36''$, $\delta_r - \delta_0 = -43''$, Fig. 1d). The identification is thus doubtful and the galaxy is, in any case, not a member of Abell 779 according to Hintzen *et al.* (1978). The radio peak lies 9″ E and 4″ N of an $18^m.5$ stellar object ; these displacements are probably too large for identification with the radio source.

5. **Source count.** — From our observations of Abell 779 and Abell 1314 we have derived the differential radio source count with respect to flux density. Since the fields were chosen primarily to study cluster radio galaxies, the 6 sources (Table V) which are possibly or probably associated with cluster galaxies were first eliminated from the radio source list. Next, four sources whose peak map flux densities are in the range 4-5 × r.m.s. (and thus are not included in table II or III) but whose *integrated* map flux densities are above 10 mJy were added to the list of sources. For each source we then calculated the maximum radius from the field center at which the radio source could have been detected. This radius is a function of flux density because of the effects of the power pattern $P(R)$ of the individual antennas. For each source, the inverse of the corresponding area of sky (in sterad) was taken and these inverses summed for sources in the sky flux density ranges 10 to 15.5 mJy, 15.5 to 24.0 mJy... where the lowest flux density limit of the ith range is given by the equation

$$S_i = 10.0(1.55)^{i-1}, \quad i = 1, 2, 3, \dots .$$

This procedure was performed separately for tables II and III and the two values of dN/dS for each flux density range were averaged.

There are a number of well known problems in such a derivation of source counts (see e.g. Valentijn 1980 for a recent summary). Firstly, it was assumed that all radio sources in the field are unrelated ; no correction was applied for possible source associations. Secondly, we applied a correction to the counts for the systematic effects of noise, by means of an extrapolation of the correction factors given in table II of Murdoch *et al.* (1973) to an integral count slope of 0.8. The largest correction needed for this effect was only 13 % for the lowest flux density bin; in all the other bins it is much smaller. Thirdly, some extended sources with peak map flux densities below the flux limit but total fluxes above it will have been missed. It is felt that, because of the rather small number (18 %, after exclusion of cluster members) of resolved sources in our survey, this effect may probably be neglected in comparison with the other errors, so no correction was applied.

The results are given in table VI and figure 2. The format of table VI is:

Column 1 : The range of sky flux density.
Column 2 : The number of radio sources in that range of sky flux density.
Column 3 : The (differential) source count before correction for the effects of noise.
Column 4 : The (differential) source count after correction for the effects of noise, with its r.m.s. error. The error quoted represents only that due to the finite number of radio sources in each bin.

The power law

$$dN/dS = 1039\, S_{\mathrm{Jy}}^{-1.94}\ \mathrm{sterad}^{-1}\ \mathrm{Jy}^{-1}$$

is also drawn on figure 2. This provides a reasonable overall fit, but lies well above the data in the range 89.5-215 mJy. However, in view of the small numbers of radio sources involved in this flux density range, the significance of the discrepancy is doubtful. The above power law is somewhat steeper than those derived earlier from WSRT 610 MHz surveys (e.g. Valentijn *et al.* 1977; Willis *et al.*, 1977; Valentijn, 1980). Also shown in figure 2 is the source count at 408 MHz from the 5C 5 survey of radio sources (Pearson, 1975), after the flux densities have been simply scaled to 610 MHz assuming a spectral index $\alpha = 0.70$ ($S \propto \nu^{-\alpha}$). The agreement with the 5C 5 counts is excellent except in the region noted above where our counts are depressed. This agreement suggests there are few (less than 7) or no radio sources associated with Abell 779 or Abell 1314 which are identified with faint galaxies or have no optical identification. A similar result has been found for the Coma cluster by Valentijn *et al.* (1977).

Acknowledgements. — The Westerbork Synthesis Radio Telescope is operated by the Netherlands Foundation for Radio Astronomy (SRZM) with the financial support of the Netherlands Organization for Pure Research (ZWO). We thank the Royal Greenwich Observatory for use of its facilities. Part of this work was done while JPV was at Queens University at Kingston, Ontario and ASW at the University of Sussex.

References

BAARS, J. W. M., BRUGGE, J. F. van der, CASSE, J. L., HAMAKER, J. P., SONDAAR, L. H., VISSER, J. J., WELLINGTON, K. J. : 1973, *Proc. Inst. Elec. Electron Eng.* **61**, 1258.
BERGAMINI, R., BRACCESI, A., COLLA, G., FANTI, C., FANTI R., FICARRA, A., FORMIGGINI, L., GANDOLFI, E., GIOIA, I., LARI, C., MARANO, B., PADRIELLI, L., TOMASI, P., VIGOTTI, M. : 1973, *Astron. Astrophys.* **23**, 195.
COLEMAN, G. D., HINTZEN, P., SCOTT, J. S., TARENGHI, M. : 1976, *Nature* **262**, 476.
FOMALONT, E. B., BRIDLE, A. H. : 1978, *Mon. Not. Roy. Astron. Soc.* **182**, 1P.
GRUEFF, G., VIGOTTI, M. : 1972, *Astron. Astrophys. Suppl. Ser.* **6**, 1.
HARRIS, D. E., KAPAHI, V. K., EKERS, R. D. : 1980, *Astron. Astrophys. Suppl. Ser.* **39**, 215.
HARRIS, D. E., MILEY, G. K. : 1978, *Astron. Astrophys. Suppl. Ser.* **34**, 117.
HINTZEN, P., OEGERLE, W. R., SCOTT, J. S. : 1978, *Astron. J.* **83**, 478.
HÖGBOM, J. A. : 1974, *Astron. Astrophys. Suppl. Ser.* **15**, 417.
HÖGBOM, J. A., BROUW, W. N. : 1974, *Astron. Astrophys.* **33**, 289.
JAFFE, W. J., PEROLA, G. C., VALENTIJN, E. A. : 1976, *Astron. Astrophys.* **49**, 179.
MCEWAN, N. J., BROWNE, I. W., CROWTHER, J. H. : 1975, *Mem. Roy. Astron. Soc.* **80**, 1.
MURDOCH, H. S., CRAWFORD, D. F., JAUNCEY, D. L. : 1973, *Astrophys. J.* **183**, 1.
OWEN, F. N. : 1974, *Astron. J.* **79**, 427.
PEARSON, T. J. : 1975, *Mon. Not. Roy Astron. Soc.* **171**, 475.
VALENTIJN, E. A., PEROLA, G. C., JAFFE, W. J. : 1977, *Astron. Astrophys. Suppl. Ser.* **28**, 333.
VALENTIJN, E. A. : 1980, *Astron. Astrophys.* **89**, 234.
VALLÉE, J. P., BRIDLE, A. H., WILSON, A. S. : 1981, *Astrophys. J.* **250**, 66.
VALLÉE, J. P., WILSON, A. S. : 1976, *Nature*, **259**, 451.
VALLÉE, J. P., WILSON, A. S., van der LAAN, H. : 1979, *Astron. Astrophys.* **77**, 183.
WILD, J. P. : 1970, *Austr. J. Phys.* **23**, 113.
WILLIS, A. G., OOSTERBAAN, C. E., de RUITER, H. R. : 1976, *Astron. Astrophys. Suppl. Ser.* **25**, 453.
WILLIS, A. G., OOSTERBAAN, C. E., LE POOLE, R. S., de RUITER, H. R., STROM, R. G., VALENTIJN, E. A., KATGERT, P., KATGERT-MERKELIJN, J. K. : 1977, In I.A.U. Symposium Nr. 46 « *Radio Astronomy and Cosmology* », (Reidel, Dordrecht, Netherlands), p. 39.
WILSON, A. S., VALLÉE, J. P. : 1977, *Astron. Astrophys.* **58**, 79.
ZWICKY, F., HERZOG, E. : 1963, *Catalogue of Galaxies and of Clusters of Galaxies, III,* Calif. Inst. Tech., Pasadena, U.S.A.

TABLE I. — *Instrumental Parameters at 610 MHz.*

Cluster	Abell 779	Abell 1314
Field Center, RA (1950.0) Dec (1950.0)	$9^h16^m00^s$ +34°00'00"	$11^h32^m00^s$ +49°20'00"
Date of Observation	Aug. 1974	Aug. 1974
Observing time (hours)	1 x 12	1 x 12
Separation 9-A (m)	72	72
Spacing Increment (m)	72	72
Maximum Baseline (m)	1440	1440
Synthesised HPBW, RA x Dec (arc sec)	52 x 93	52 x 69
Radius of first grating ring, RA x Dec (arc min)	24 x 43	24 x 32
R.m.s. noise $\left(\text{mJy (beam area)}^{-1}\right)$	1.8	2.0

TABLE II. — *A779 Survey (cluster and background).*

(1) Name	(2) RA(1950)	s.d.	(3) Dec(1950)	s.d.	(4) Atten.	(5) S_{610} (mJy)	s.d. (mJy)	(6) Struc-ture
0910+33W1	$09^h10^m24^s80$	0^s42	+33°59'14".5	09".3	09.19	80.4	19.3	U
0912+33W1	09 12 10.73	0.44	+33 44 10.7	09.7	02.90	49.1	09.1	R
0912+33W2	09 12 12.92	0.12	+33 12 17.4	02.7	07.84	216.	28.	U
0912+34W1	09 12 18.62	0.08	+34 14 03.7	01.8	02.62	407.	37.	R
0912+33W3	09 12 28.89	0.11	+33 43 03.0	02.6	02.53	73.9	08.0	U
0912+33W4	09 12 43.76	0.42	+33 58 20.6	09.3	01.99	18.1	03.9	U
0913+33W1	09 13 08.49	0.08	+33 48 17.1	01.8	01.79	359.	27.	R
0913+34W1	09 13 09.62	0.10	+34 48 17.8	02.3	04.74	150.	18.	U
0913+33W2	09 13 37.47	0.13	+33 51 09.6	03.0	01.48	37.1	03.6	U
0913+34W2	09 13 43.73	0.26	+34 47 57.1	05.9	03.76	48.9	08.4	U
0913+34W3	09 13 50.26	0.35	+34 12 20.8	07.7	01.43	14.7	02.7	U
0913+34W4	09 13 52.45	0.24	+34 43 49.7	05.2	03.02	43.6	06.8	U
0913+33W3	09 13 58.63	0.09	+33 44 42.8	02.0	01.43	56.0	03.9	U
0914+34W1	09 14 11.98	0.08	+34 59 19.0	01.8	05.95	1637.	187.	U
0914+34W2	09 14 18.49	0.09	+34 08 03.2	02.1	01.23	46.4	02.9	U
0914+33W1	09 14 19.26	0.36	+33 11 30.8	08.0	03.29	32.7	06.7	U
0914+34W3	09 14 20.79	0.10	+34 03 58.9	02.2	01.20	41.8	02.7	U
0914+33W2	09 14 35.18	0.22	+33 42 53.9	05.0	01.28	20.0	02.5	U
0914+33W3	09 14 46.84	0.19	+33 57 54.5	03.8	01.10	27.9	03.1	R
0915+34W1	09 15 06.22	0.24	+34 33 33.1	05.2	01.67	24.1	03.5	U
0915+34W2	09 15 08.52	0.30	+34 24 03.9	06.7	01.33	31.9	03.9	R
0915+33W1	09 15 20.23	0.17	+33 52 18.5	03.7	01.05	21.4	02.0	U
0915+34W3	09 15 22.76	0.08	+34 26 10.8	01.9	01.36	56.8	03.7	U
0915+33W2	09 15 43.50	0.10	+33 21 29.6	02.2	01.86	62.6	05.9	U
0915+33W3	09 15 46.04	0.37	+33 40 06.6	08.4	01.18	11.4	02.2	U
0915+33W4	09 15 46.38	0.10	+33 57 34.6	02.2	01.00	34.2	01.9	U
0915+33W5	09 15 55.80	0.45	+33 33 40.5	09.9	01.33	11.4	02.4	U
0915+33W6	09 15 58.74	0.48	+33 45 46.5	10.6	01.08	14.5	02.5	U
0916+33W1	09 16 06.30	0.08	+33 37 23.1	01.8	01.23	80.0	03.9	U
0916+34W1	09 16 09.83	0.08	+34 31 05.0	01.8	01.49	218.	15.	U
0916+34W2	09 16 12.74	0.08	+34 13 33.3	01.8	01.08	461.	13.	R
0916+33W2	09 16 20.81	0.08	+33 42 14.5	01.8	01.14	169	06.	U
0916+33W3	09 16 32.97	0.10	+33 42 01.9	02.3	01.16	37.8	02.5	U
0916+33W4	09 16 33.95	0.17	+33 31 40.1	03.8	01.42	28.2	02.9	U
0916+34W3	09 16 34.08	0.72	+34 08 35.6	16.1	01.05	17.3	02.9	R
0916+33W5	09 16 40.93	0.23	+33 41 25.7	05.0	01.18	17.8	02.2	U

TABLE II *(continued).*

(1)	(2)		(3)		(4)	(5)		(6)
0916+33W6	09 16 43.05	0.30	+33 57 29.8	06.6	01.03	12.2	01.9	U
0916+33W7	09 16 49.42	0.09	+33 07 58.3	02.1	03.32	207.	21.	R
0916+34W4	09 16 53.08	0.19	+34 03 48.2	04.3	01.05	18.7	01.9	U
0917+34W1	09 17 05.04	0.43	+34 22 42.7	09.5	01.33	11.7	02.5	U
0917+34W2	09 17 13.54	0.38	+34 49 48.1	08.5	03.16	30.3	06.4	U
0917+33W1	09 17 18.81	0.08	+33 25 27.8	01.8	01.83	228.	18.	U
0917+33W2	09 17 18.98	0.36	+33 16 05.6	08.0	02.51	25.0	05.0	U
0917+34W3	09 17 27.35	0.32	+34 27 54.6	07.2	01.57	17.4	03.1	U
0918+33W1	09 18 29.07	0.14	+33 30 24.1	03.1	02.15	49.8	06.9	R
0918+33W2	09 18 34.18	0.17	+33 41 35.7	03.8	01.76	35.1	04.1	U
0918+33W3	09 18 49.10	0.08	+33 36 59.9	01.8	02.08	154.	13.	R
0919+34W1	09 19 09.83	0.14	+34 18 43.5	03.1	02.19	53.1	07.1	R
0919+33W1	09 19 11.92	0.43	+33 17 31.7	09.4	04.41	39.1	09.0	U
0919+33W2	09 19 21.96	0.30	+33 43 35.0	06.5	02.34	27.4	04.8	U
0919+34W2	09 19 32.75	0.33	+34 22 54.7	07.4	02.81	45.6	07.3	U
0919+34W3	09 19 40.66	0.23	+34 07 52.5	05.5	02.46	57.0	08.1	R
0920+34W1	09 20 00.90	0.08	+34 27 47.1	01.8	04.05	488.	51.	U
0920+34W2	09 20 29.76	0.27	+34 06 44.3	05.7	03.91	53.0	08.9	U
0920+34W3	09 20 38.14	0.30	+34 30 47.8	06.8	06.69	77.2	15.0	U

TABLE III. — *A1314 Survey (cluster and background).*

(1) Name	(2) RA(1950)	s.d.	(3) Dec(1950)	s.d.	(4) Atten.	(5) S_{610} (mJy)	s.d. (mJy)	(6) Struc-ture
1125+49W1	$11^h25^m55^s18$	0^s30	+49°27'43".0	03".7	04.78	76.7	12.7	U
1127+48W1	11 27 34.04	0.18	+48 56 05.6	02.4	02.85	71.2	08.7	U
1127+49W1	11 27 34.37	0.14	+49 27 45.1	01.9	02.23	70.2	08.6	R
1127+49W2	11 27 48.60	0.40	+49 17 34.5	05.1	02.01	25.0	04.5	U
1127+49W3	11 27 59.97	0.29	+49 40 08.0	03.7	02.22	37.3	05.4	U
1128+49W1	11 28 18.39	0.11	+49 12 39.0	01.4	01.76	88.1	07.7	R
1128+48W1	11 28 28.96	0.21	+48 45 03.1	02.7	02.79	61.0	08.0	U
1129+50W1	11 29 28.31	0.48	+50 04 23.2	06.2	02.96	32.1	06.7	U
1129+49W1	11 29 54.86	0.53	+49 43 59.2	06.9	01.50	14.7	03.2	U
1130+49W1	11 30 07.42	0.49	+49 25 12.3	06.4	01.16	12.3	02.4	U
1130+49W2	11 30 15.34	0.51	+49 12 27.8	06.5	01.15	18.3	02.9	U
1130+48W1	11 30 22.84	0.32	+48 50 01.5	04.1	01.61	24.0	03.6	U
1130+49W3	11 30 23.84	0.36	+49 30 05.5	04.6	01.15	15.8	02.4	U
1130+50W1	11 30 29.60	0.10	+50 25 14.9	01.3	07.56	1508.	178.	U
1130+49W4	11 30 30.69	0.15	+49 33 53.6	02.0	01.18	35.3	02.7	U
1130+49W5	11 30 33.76	0.13	+49 31 52.5	01.7	01.15	38.8	02.6	U
1130+49W6	11 30 37.74	0.40	+49 05 38.7	05.1	01.17	14.9	02.4	U
1130+48W2	11 30 38.86	0.21	+48 20 30.7	02.7	05.14	113.	16.	U
1130+49W7	11 30 40.30	0.10	+49 18 48.5	01.3	01.07	66.7	02.8	U
1130+49W8	11 30 42.06	0.41	+49 42 13.4	05.3	01.31	26.8	04.1	R
1130+49W9	11 30 44.68	0.36	+49 47 10.6	04.7	01.44	18.5	03.0	U
1130+48W3	11 30 48.69	0.26	+48 58 53.0	03.3	01.27	22.8	02.7	U
1131+49W1	11 31 05.20	0.16	+49 15 38.3	02.1	01.04	53.9	03.4	R
1131+49W2	11 31 16.13	0.36	+49 12 50.4	04.6	01.04	14.5	02.1	U
1131+49W3*	11 31 16.22	0.10	+49 19 20.0	02.0	01.02	55.9	02.3	U
1131+49W4	11 31 16.27	0.04	+49 20 19.3	02.0	01.02	1456.	73.	C
1131+49W5	11 31 23.45	0.30	+49 11 24.0	03.9	01.04	16.5	02.1	U
1131+50W1	11 31 55.91	0.29	+50 01 51.4	03.6	02.07	34.5	05.0	U
1131+49W6	11 31 57.34	0.40	+49 31 05.6	05.1	01.05	13.1	02.1	U
1132+49W1	11 32 03.46	0.27	+49 47 29.8	03.4	01.36	23.8	03.0	U
1132+49W2	11 32 03.90	0.04	+49 13 57.8	02.0	01.01	1058.	101.	C
1132+49W3	11 32 06.50	0.10	+49 21 17.0	01.3	01.00	58.7	02.2	U
1132+49W4	11 32 11.58	0.24	+49 55 24.5	03.0	01.68	33.3	04.2	U
1132+48W1	11 32 13.78	0.41	+48 53 12.0	05.3	01.35	16.3	02.8	U

TABLE III *(continued)*.

(1)	(2)	(3)	(4)	(5)		(6)
1132+49W5	11 32 15.74 0.40	+49 09 59.2 05.2	01.04	12.8	02.1	U
1132+49W6	11 32 18.65 0.27	+49 28 23.8 03.5	01.03	26.9	03.2	R
1132+50W1	11 32 22.07 0.10	+50 08 21.1 01.3	02.69	320.	30.	U
1132+49W7	11 32 24.90 0.57	+49 31 14.0 07.4	01.06	09.8	02.1	U
1132+49W8	11 32 30.12 0.16	+49 14 33.2 02.1	01.02	29.0	02.1	U
1132+49W9	11 32 33.01 0.69	+49 31 35.7 08.9	01.07	09.1	02.2	U
1132+49W10	11 32 50.69 0.53	+49 43 27.5 06.9	01.29	12.6	02.6	U
1133+48W1	11 33 11.45 0.36	+48 25 54.7 04.8	03.66	50.0	08.9	U
1133+48W2	11 33 44.27 0.28	+48 19 38.5 03.6	05.76	97.1	15.9	U
1134+49W1	11 34 04.30 0.13	+49 08 10.0 01.7	01.25	44.5	03.1	U
1134+48W1	11 34 27.46 0.14	+48 42 04.2 01.8	02.33	74.5	07.9	U
1134+49W2	11 34 39.39 0.39	+49 41 24.8 04.9	01.59	20.6	03.5	U
1134+49W3	11 34 44.20 0.47	+49 07 21.4 06.1	01.44	15.8	03.0	U
1134+49W4	11 34 51.79 0.24	+49 34 38.2 03.0	01.50	29.8	03.6	U
1135+49W1	11 35 20.26 0.31	+49 15 32.4 04.0	01.56	24.1	03.5	U
1135+50W1	11 35 35.24 0.17	+50 07 00.7 02.2	04.39	119.	15.	U
1135+48W1	11 35 36.64 0.42	+48 20 51.8 05.4	09.02	109.	23.	U
1135+49W2	11 35 43.86 0.15	+49 45 16.6 01.9	02.25	79.2	08.3	U
1136+49W1	11 36 13.15 0.59	+49 07 45.2 07.6	02.17	44.2	07.3	R
1136+50W1	11 36 34.88 0.42	+50 16 39.4 05.4	10.86	129.	27.	U
1136+49W2	11 36 37.88 0.10	+49 15 27.6 01.3	02.38	148.	14.	U
1137+49W1	11 37 16.07 0.10	+49 19 05.5 01.3	03.08	477.	42.	R

*The source 1131+49W3 is not resolved from 1131+49W4 (IC 708) in the present observations. Its flux density at λ49 cm has been obtained by extrapolation from λ6 and 21 cm (see Vallée and Wilson, 1976).

TABLE IV. — *Resolved (R) or Complex (C) Sources.*

Resolved (R) or Complex (C) Sources

(1) Name	(2) PA (°)	(3) θ_G (")	(4) $\theta_{G,min}$ (")	(5) θ_{dp} (")
0912+33W1	35	60	–	45
0912+34W1	80	45	–	34
0913+33W1	61	22	–	18
0914+33W3	8	48	–	40
0915+34W2	168	116	–	75
0916+34W2	95	27	–	23
0916+34W3	148	81	44	55
0916+33W7	15	44	–	37
0918+33W1	69	73	41	46
0918+33W3	102	36	–	29
0919+34W1	128	48	–	37
0919+34W3	154	52	–	41
1127+49W1	128	45	36	34
1128+49W1	176	42	–	34
1130+49W8	28	45	–	35
1131+49W1	6	52	–	40
1131+49W4 = IC 708	See Vallée and Wilson (1976)			
1132+49W2 = IC 711	See Vallée and Wilson (1976)			
1132+49W6	136	46	–	35
1136+49W1	174	90	–	58
1137+49W1	152	22	–	18

TABLE V. — *Probable or Possible Cluster Members.*

Probable or Possible Cluster Members

Name	m_p [(a)] (m)	Cluster	Galaxy Type	M_p (m)	Monochromatic Power P_{610} (10^{24} W/Hz)	Radio Extent (kpc)	$\alpha_r-\alpha_o$ (")	$\delta_r-\delta_o$ (")	Comments
0916+33W6=NGC2831/2	14.7	A779	Ell.	-21.0	0.03	∼ 38	+06. [(b)]	+08. [(b)]	See text and Figure 1c
0918+33W3	14.6	A779	Ell.	-21.0	0.32	∼ 23	-04.	+07.	See Figure 1e
1130+49W7 [(c)]	--	A1314?	Sp.	--	--	--	+04.	-01.	
1131+49W4=IC708	14.2	A1314	Ell.	-22.3	6.7	∼ 80	-01. [(d)]	+01. [(d)]	See also Vallée and Wilson (1976), Wilson and Vallée (1977).
1132+49W2=IC711	15.2	A1314	Ell.	-21.3	4.8	∼820	-00. [(d)]	+01. [(d)]	
1132+49W3=IC712	14.8	A1314	Ell.	-21.7	0.27	<27	+04.	+03.	

[(a)] From Zwicky and Herzog (1963).

[(b)] Offsets of radio source 0916+33W6 are given w.r.t. NGC2831.

[(c)] To our knowledge, no redshift has been measured for this galaxy. The redshifts for the remainder are given by Hintzen et al. (1978) for Abell 779 and by Coleman et al. (1978) for Abell 1314.

[(d)] The offsets for IC708 and IC711 refer to the difference of position between the nuclear radio component and the centroid of the optical galaxy (Vallée and Wilson 1976).

TABLE VI. — *Source Counts.*

Source Counts

S_{sky}^{610} (Jy)	N	$(dN/dS)_{uncorr}$ (Ster^{-1} Jy^{-1})	$(dN/dS)_{corr}$ (Ster^{-1} Jy^{-1})
0.010 - 0.0155	14	6.7×10^6	5.9×10^6 ± 1.6
0.0155 - 0.0240	19	2.7×10^6	2.5×10^6 0.6
0.0240 - 0.0372	21	1.1×10^6	1.1×10^6 0.2
0.0372 - 0.0577	21	4.9×10^5	4.8×10^5 1.1
0.0577 - 0.0895	12	1.6×10^5	1.5×10^5 0.4
0.0895 - 0.139	5	3.6×10^4	3.3×10^4 1.5
0.139 - 0.215	4	1.8×10^4	1.7×10^4 0.9
0.215 - 0.333	4	1.1×10^4	1.1×10^4 0.6
0.333 - 0.516	5	9.1×10^3	9.0×10^3 4.0

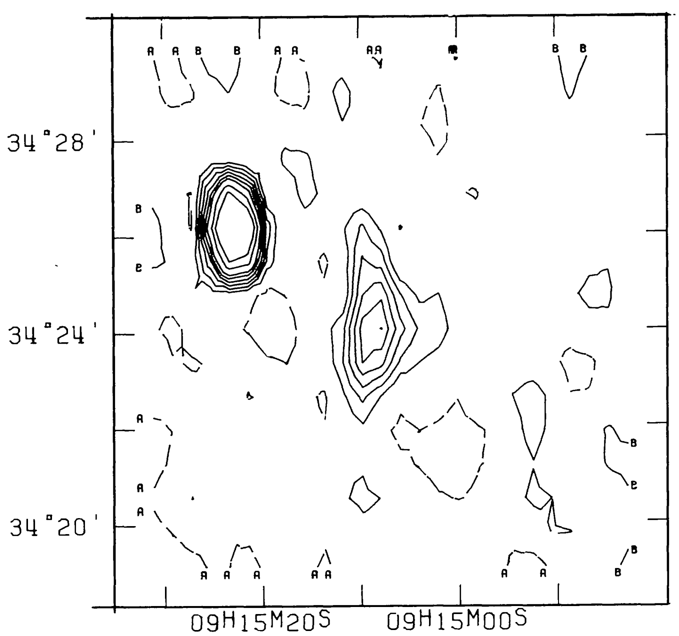

FIGURE 1a.

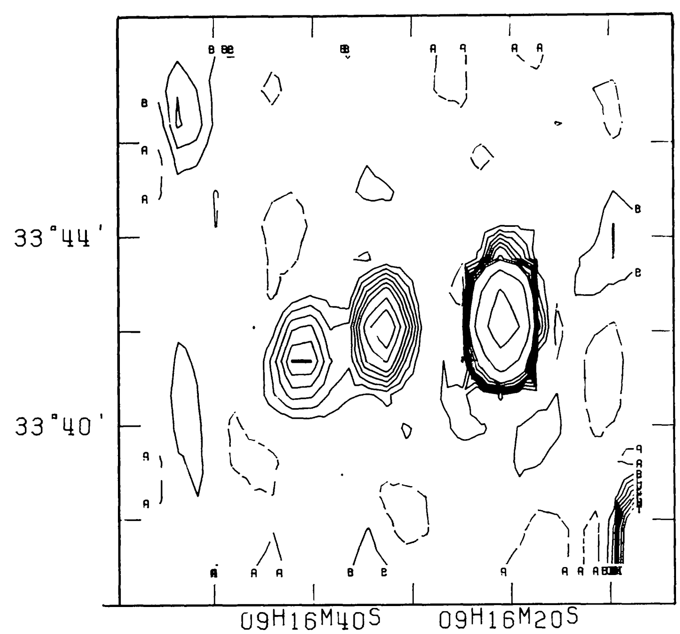

FIGURE 1b.

FIGURE 1. — Contour maps at λ 49 cm for some extended and/or closely grouped sources. Contour levels are in *map* flux density, at : − 2.5 (dashed), + 2.5, 5, 7.5, 10, 12.5, 15, 20, 25, 50, 100, 150, 200, 300, 400 and 500 mJy (beam area)$^{-1}$. To convert these levels into sky flux density for a given source, they should be multiplied by the attenuation (column 4 in tables II and III). The HPBW is 52″ × 93″ for A779 and 52″ × 69″ for A1314.

a) 0915 + 34W2 (center) and 0915 + 34W3 (east).

b) 0916 + 33W2 (west), 0916 + 33W3 (center), and 0916 + 33W5 (east).

c) 0916 + 33W6 (center). The three crosses represent the galaxies (from west to east) NGC 2830, NGC 2831 and NGC 2832 (see table V and section 4).

d) 0916 + 33W7. The northern cross marks an 15^{m}.3 galaxy, while the southern cross marks an 18^{m}.5 stellar object (see Table II and section 4).

e) 0918 + 33W3 (center) and 0918 + 33W2 (west). The cross marks a 14^{m}.6 cluster member (Table V).

f) 1128 + 49W1.

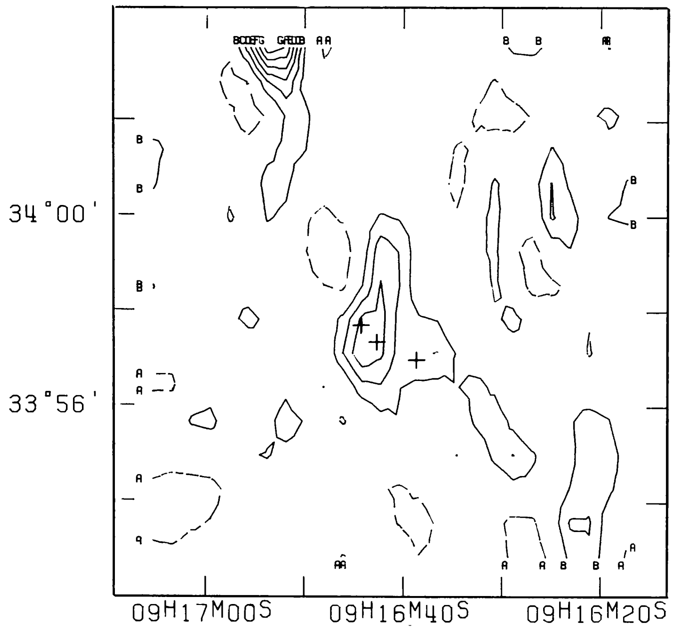

FIGURE 1c.

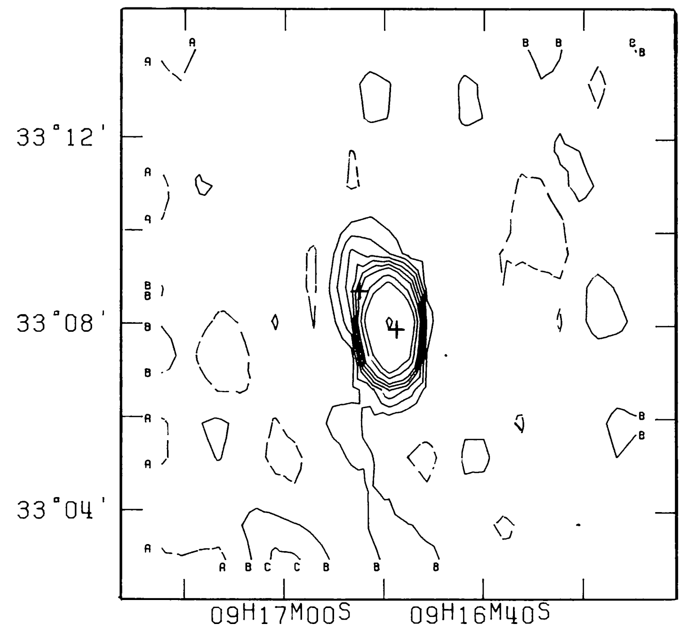

FIGURE 1d.

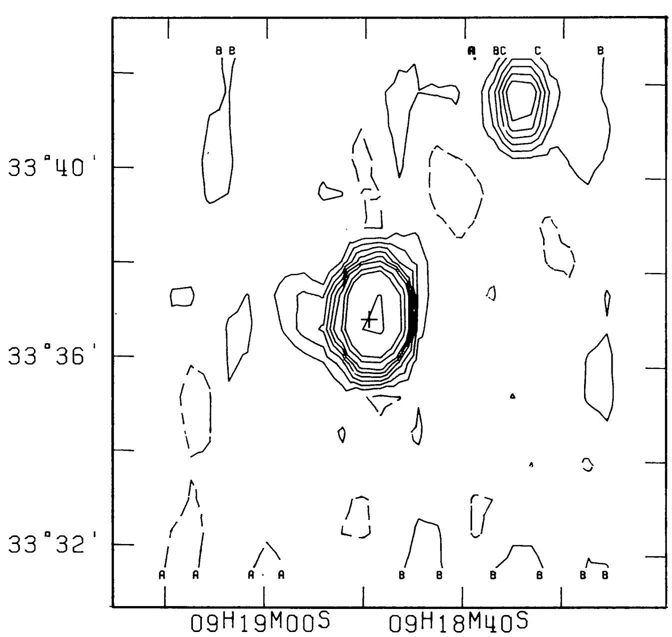

FIGURE 1e.

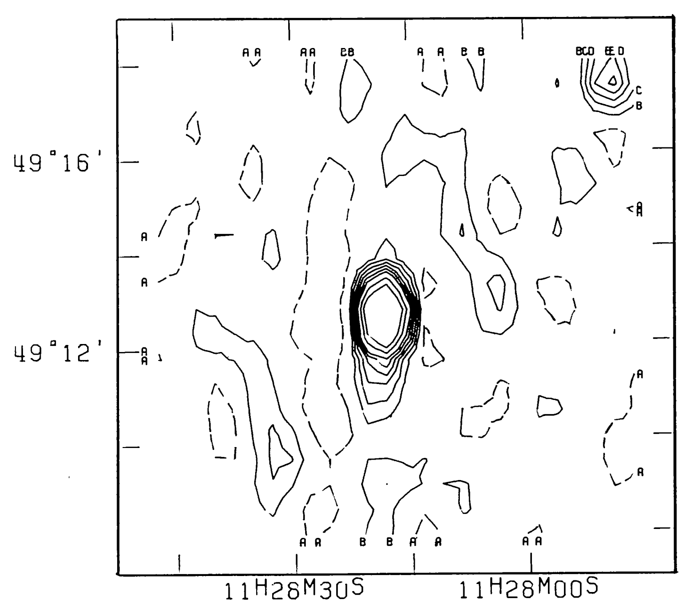

FIGURE 1f.

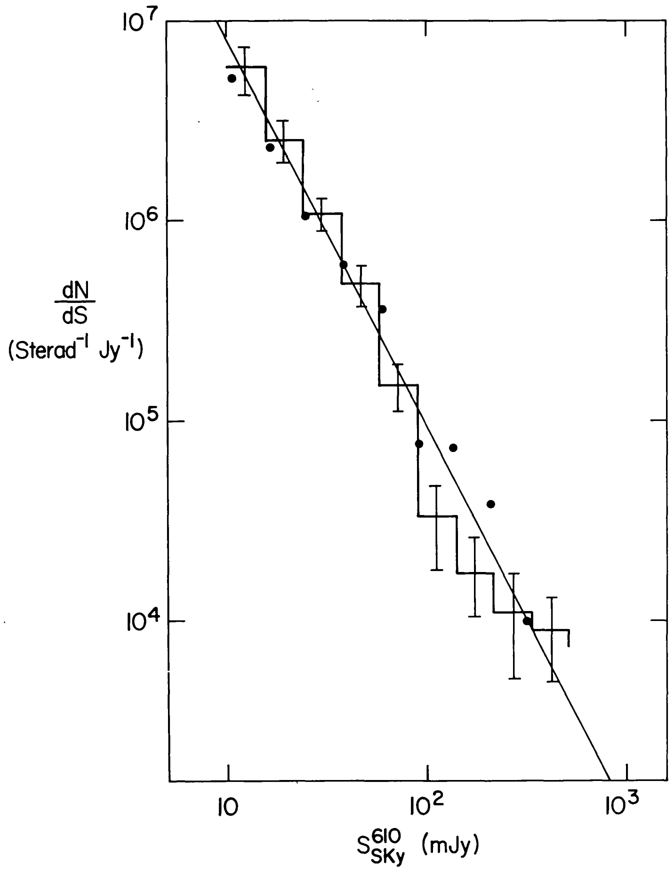

FIGURE 2. — The differential background source count dN/dS (sterad^{-1}Jy^{-1}) at 610 MHz, as a function of sky flux density (mJy), plotted on a log-log scale. Black symbols are for the non-cluster field of Pearson (1975) at 408 MHz, corrected to 610 MHz assuming a spectral index of 0.7.